Journal Pre-proof

Graphene oxide bioaugmentation of E. coli enables nutrient-free, light-independent methylene blue removal via spontaneous bio–nano flocculation

Valentina Palmieri , Valeria Ferrara , Caterina Perfili , Ginevra Friggeri , Giulia Artemi , Giordano Perini , Alberto Augello , Francesca Sciandra , Francesco Amato , Andrea Giacomo Marrani , Claudio Catalano , Umberto Romeo , Guido Caldarelli , Marco De Spirito , Massimiliano Papi

PII: S2468-0230(26)01944-9
DOI: https://doi.org/10.1016/j.surfin.2026.110367
Reference: SURFIN 110367

To appear in: *Surfaces and Interfaces*

Received date: 4 June 2026
Revised date: 31 July 2026
Accepted date: 10 August 2026

Please cite this article as: Valentina Palmieri , Valeria Ferrara , Caterina Perfili , Ginevra Friggeri , Giulia Artemi , Giordano Perini , Alberto Augello , Francesca Sciandra , Francesco Amato , Andrea Giacomo Marrani , Claudio Catalano , Umberto Romeo , Guido Caldarelli , Marco De Spirito , Massimiliano Papi , Graphene oxide bioaugmentation of E. coli enables nutrient-free, light-independent methylene blue removal via spontaneous bio–nano flocculation, *Surfaces and Interfaces* (2026), doi: https://doi.org/10.1016/j.surfin.2026.110367

Graphene oxide bioaugmentation of *E. coli* enables nutrient-free, light-independent methylene blue removal via spontaneous bio–nano flocculation

Valentina Palmieri[1,*], Valeria Ferrara[2], Caterina Perfili[3], Ginevra Friggeri[3], Giulia Artemi[3], Giordano Perini[3], Alberto Augello[2], Francesca Sciandra[4], Francesco Amato[5], Andrea Giacomo Marrani[5], Claudio Catalano[6], Umberto Romeo[6], Guido Caldarelli[1], Marco De Spirito[2,3#], Massimiliano Papi[2,3#]

[1] Istituto dei Sistemi Complessi, CNR, Via dei Taurini 19, 00185 Rome, Italy

[2] Università di Roma "La Sapienza", p.le A. Moro 5, I-00185 Rome, Italy

[3] Dipartimento di Neuroscienze, Università Cattolica del Sacro Cuore, Largo Francesco Vito 1, 00168 Rome, Italy

[4] Istituto di Scienze e Tecnologie Chimiche, SCITEC- CNR, c/o Università Cattolica del Sacro Cuore, Largo Francesco Vito 1, 00168, Rome, Italy

[5]Dipartimento di Chimica, Università di Roma "La Sapienza", p.le A. Moro 5, I-00185 Rome, Italy

[6] Dipartimento di Scienze Odontostomatologiche e Maxillofacciali, Via Caserta 6, I-00161 Rome, Italy

#Co-last authors

Abstract

The contamination of water bodies with dye pollutants, particularly methylene blue (MB), represents a significant environmental challenge due to the widespread use in industries such as textiles, pharmaceuticals, and cosmetics. Effective removal of MB from wastewater is essential to prevent ecological damage and safeguard human health. Various techniques have been explored globally for dye segregation, including adsorption methods utilizing light activated nanomaterials such as graphene oxide combined with catalytic metal atoms and bioremediation employing bacteria. Enzymes are also widely studied but are prone to biocatalyst deactivation due to denaturation. Also, some bacteria, such as *E.coli*, are sensitive to MB and this represents a limiting step for highly concentrated MB solutions. Among these methods a light independent self-sustained strategy has not been developed. Indeed, even if carbon materials such as graphene oxide are efficient, their efficacy in the absence of light exposure is limited.

In this paper, we demonstrate a novel spontaneous flocculation method combining graphene oxide and *E. coli* bacteria for the efficient removal of MB from aqueous solutions. Spectroscopic analysis confirms significant dye removal efficacy through the formation of flocs, highlighting a synergistic interaction between graphene oxide and bacterial cells. *E. coli* is considered a non-decolorizer bacterium but in presence of graphene oxide cells is trapped and water decolorization is fostered on the surface of the nanomaterial. We also demonstrate that infrared light (805 nm) can be used to inactivate bacteria thanks to an enhanced NIR adsorption of MB deposited on graphene oxide flakes.

The detoxification method of wastewater containing methylene blue, based exclusively on the use of graphene oxide and without the addition of iron- or copper-based metallic particles, prevents the introduction of additional inorganic contaminants into the environment. Our findings not only validate the effectiveness of this combined approach but also suggest its potential for scalable applications in wastewater treatment, providing an innovative and eco-friendly solution to address global water pollution challenges.

Keywords: Graphene oxide; *E. coli*; Methylene blue; Wastewater treatment; Bio–nano flocculation; Dye removal; Bioremediation

1. Introduction

The textile industry is among the most polluting industrial sectors worldwide (1). Its production chain consumes enormous amounts of freshwater, employs hazardous chemicals and synthetic dyes, releases microplastic fibres, and relies heavily on non-renewable resources. These facts highlight the urgent need for sustainable technologies across the textile production cycle to minimize its environmental footprint (2). In addition to their environmental burden, many synthetic dyes exhibit carcinogenic, mutagenic, and toxic effects on humans and animals. These dyes are chemically recalcitrant, persist in ecosystems, and may undergo biomagnification through the food chain (3,4). Methylene blue (MB) is one of the most widely used synthetic dyes in textile processing. MB is non-biodegradable, persistent, and has been reported to cause severe toxicological effects including oxidative stress, haematological alterations such as methemoglobinemia, and neurotoxicity (5). Given its widespread use, the environmental release of MB represents a major health and ecological concern.

Conventional physicochemical treatments for textile effluents—including adsorption on activated carbon, coagulation, reverse osmosis, ozonation, photocatalysis, Fenton-based oxidation, electrochemical oxidation, and membrane filtration—are effective for dye removal but often require high energy input, expensive reagents, or complex operating conditions. In addition, several of these processes generate secondary waste streams, such as toxic sludge or spent adsorbents, requiring further disposal or regeneration, thereby increasing the overall environmental and economic costs (6–8). In recent years, biological approaches have gained increasing attention as greener alternatives. Bacteria, fungi, microbial consortia, and isolated enzymes have been investigated for dye removal, either alone or in combination with physicochemical methods, providing cost-effective and environmentally friendly solutions (2,9,10).

The biodegradation of azo dyes by bacteria generally proceeds through two distinct stages. First, the azo bonds undergo reductive cleavage, producing aromatic amines, which are often toxic and persistent. In the second stage, these aromatic amines are further broken down. While the initial cleavage can occur under both aerobic and anaerobic conditions, the effective degradation of the resulting aromatic amines takes place predominantly under aerobic conditions. Therefore, the most effective strategy for treating industrial effluents contaminated with azo compounds is an integrated process that combines anaerobic and aerobic steps, ensuring both efficient dye removal and the minimization of environmental and human health risks (11).

However, the efficiency of microbial removal is strongly influenced by environmental and nutritional factors, including pH, temperature, dissolved oxygen, organic matter, metals, and co-pollutants (9).

Biological approaches are frequently limited by bacterial sensitivity to toxic dyes, the need for nutrients, long treatment times, and strong dependence on environmental parameters such as pH, temperature, and oxygen availability. To overcome these limitations, strategies such as genetic engineering to enhance resistance and expand the enzyme repertoire, enzymatic treatments, hybrid systems, and microbial flocculants have been proposed (2). Often microorganisms have to be acclimatized to compounds to obtain an efficient dye removal (12–14). Consequently, hybrid systems combining physicochemical adsorption with biological activity are increasingly being explored to exploit the advantages of both strategies while minimizing their individual limitations.

The search for bacteria capable of degrading dyes can take advantage of the “natural” selection of these organisms through bioprospecting in contaminated environments, selecting bacteria that underwent great environmental pressure, thanks to human action (15).

Escherichia coli is a widespread and adaptable microorganism, capable of surviving in challenging environments for a certain time span. However, *E. coli* itself is not highly efficient in dye removal, and it is considered a non exoelectrogen and non-decolorizer. Indeed, previous studies have shown that *E. coli* exhibits limited methylene blue removal efficiency compared to specialized dye-degrading microorganisms, highlighting its role as a weak or non-specific decolorizer (5). *E.coli* can enhance the activity of other

bacteria (16) and remains a valuable potentially ideal microorganism for environmental treatment due to its ease of cultivation and genetic manipulation (17,18).

On the material side, carbon nanomaterials such as graphene oxide (GO), the water-soluble alternative to graphene, exhibit high water dispersibility and strong pollutant adsorption properties, and have been applied to capture dyes prior to light- or photocatalysis-based deactivation (19). GO has recently emerged as a multifunctional platform capable of combining adsorption, catalytic activity, and antimicrobial effects within a single material system, enabling the simultaneous removal and transformation of contaminants (20–28).

GO has been extensively investigated as an adsorbent for MB removal owing to its large specific surface area, abundant oxygen-containing functional groups, and strong electrostatic and π–π interactions with cationic dyes. Several studies have demonstrated that the adsorption performance strongly depends on the oxidation degree and reduction state of graphene-based materials, which influence both the density of surface functional groups and the availability of graphitic domains for π–π stacking (29–32). Reduced graphene oxide generally exhibits enhanced adsorption capacity due to the restoration of aromatic domains, whereas highly oxidized GO provides improved water dispersibility and abundant adsorption sites. More recently, GO has also been explored as a metal-free photocatalytic platform for the simultaneous adsorption and light-assisted degradation of methylene blue, highlighting the potential of graphene-based materials for sustainable wastewater remediation.

GO collapses and rearranges in presence of ions and macromolecules in solution and therefore can be exploited to design both physical and chemical strategies for wastewater remediation as well as for microbial entrapment and immobilization (33–35). For instance, physical processes such as adsorption onto GO sheets allow the capture of dyes, heavy metals, and organic pollutants, while chemical methods like coagulation and flocculation promote the aggregation and subsequent removal of contaminants from aqueous solutions (36). Beyond these processes, GO also displays intrinsic catalytic and photocatalytic properties, enabling the deactivation of hazardous compounds such as methylene blue, phenolic pollutants, and even pharmaceutical residues (21). However, multi-step approaches based on photolysis often face challenges related to process complexity, costs, and incomplete removal of toxic byproducts (36).

Furthermore GO aggregation can be harnessed for a range of physical and chemical approaches to wastewater treatment (37) and biomolecules and bacterial entrapment (33). Particularly, microorganisms entrapment was demonstrated to be effective due to the binding of membranes to the hydrophilic functional groups on the material surface and is a phenomenon which is driven by concentration, ions, and lateral size of GO flakes in respect to microbial cell size (34,35,38).

Here, we propose a synergistic strategy that combines unmodified *E. coli* cells with GO aggregation to achieve efficient MB dye removal on GO surface in absence of light exposure. We demonstrate by various spectroscopy techniques an effect mediated by surface proximity of bacteria and MB. By coupling the biological adaptability of bacteria with the physicochemical adsorption properties of GO, this system aims to provide a sustainable and scalable method for the detoxification of MB. *E. coli* cells remain viable in presence of GO aggregates and MB and the process can be stopped by using Near Infrared Light (NIR) to induce hyperthermia and control bacterial growth. The underlying molecular mechanisms responsible for the observed synergistic effect remain to be elucidated and are discussed here as a future working hypothesis.

2. Materials and methods

2.1 Graphene Oxide preparation and characterization

GO (Graphenea, Spain) was used at the final concentration reported in each graph from a batch at 4 mg/mL using ultrapure water (18.2 MΩ·cm; conductivity <0.055 μS/cm) for further dilution. Samples were periodically vortexed to avoid precipitation. GO hydrodynamic properties were characterized using a Zetasizer Nano ZS (Malvern, Herrenberg, Germany). MB (Sigma Aldrich, CAS No.: 7220-79-3) has been diluted in ultrapure water at a stock solution concentration of 1 mg/mL. In Calcium containing samples a final concentration of 5 mM $CaCl_2$ was used, as described below. GO-MB aggregates were washed via

centrifugation (10000 g, 10 minutes) prior to quantify the hydrodynamic size and surface charge. Measurements were performed at a fixed detection angle of 173° with automatic attenuator settings. For each sample, three consecutive readings were taken, and the Z-average size was calculated via the Stokes–Einstein equation using cumulant analysis. Electrophoretic light scattering was employed for ζ-potential determination, with values calculated from electrophoretic mobility applying the Henry correction within Smoluchowski's model. Data acquisition and processing were conducted through the Malvern Zetasizer software. GO further characterization was reported in our previous work (39). Absorbance was evaluated by measuring Optical density (OD) spectra. Absorbance and fluorescence spectra have been recorded in a UV transparent 96 well using Cytation 3 Cell Imaging Multi-Mode Reader.

Removal efficiency was calculated from the absorbance at 610 nm of the collected supernatants according to

$$\text{Removal (\%)} = \frac{OD_0 - OD_t}{OD_0} \times 100$$

where $OD_0$is the absorbance of the initial MB solution and OD_t is the absorbance of the corresponding supernatant after a certain time of incubation.

The apparent adsorption capacity (q_e, mg g^{-1}) was then calculated as:

$$q_e = \frac{(C_0 - C_e)V}{m}$$

where V is the solution volume (L) and m is the mass of graphene oxide where C_0 and C_e are the initial and equilibrium MB concentrations (mg L^{-1}). Because the hybrid GO–*E. coli* system may involve adsorption, bio–nano flocculation, and bacterial metabolic activity simultaneously, the calculated q_e values are reported as apparent adsorption capacities.

To verify the adsorption state of methylene blue (MB) on graphene oxide (GO), the dye was desorbed from the GO surface using an ethanol/acid extraction protocol. After incubation, GO-containing pellets were collected by centrifugation and the supernatant was discarded. The pellets were then resuspended in a solution containing 50% (v/v) ethanol and 0.1 M HCl and gently mixed for 30 min at room temperature to promote disruption of the non-covalent interactions between MB and GO. Following centrifugation, the absorbance of the recovered supernatant was measured by UV–Vis spectroscopy

2.2 Bacteria cell growth and near infrared (NIR) irradiation

E. coli (ATCC strain 25922) was grown in Luria Bertani (LB) medium at 37 °C overnight, and cells were harvested via centrifugation (4000 g for 10 min) and washed three times with deionized water to remove medium residuals. The pellets were then suspended in ultrapure water to obtain a final OD of 1 corresponding to $1x10^8$ CFU/mL. Experiments with MB have been performed at 37 °C in water or in 5 mM Calcium Chloride dissolved in ultrapure water. Cell viability in controls was evaluated by the colony counting method spreading 100 μL of bacterial solution onto LB plates and letting colonies grow overnight at 37 °C. No ultrasonic treatment was performed to avoid aggregates dissolution.

To evaluate bacterial inactivation using NIR light, 72 hours after incubation samples with *E. coli*, *E-coli* and MB (31.25 μg/mL), *E.coli*- GO (100 μg/mL) or *E.coli*- GO (100 μg/mL) -MB (31.25 μg/mL) have been irradiated with a NIR laser source (805 nm) at power of 1.5 W/cm^2 (low power) or 2.5 W/cm^2 (high power) for 240 seconds, hereafter referred as medium and high power doses. Then samples have been plated on LB agar and CFU have been calculated after overnight incubation at 37°C and compared to untreated samples.

2.3 Scanning Electron Microscopy (SEM)

For morphological analysis, bacterial cells were fixed in 2.5% glutaraldehyde in phosphate-buffered saline (PBS) for 2 hours at 4 °C. Samples were then washed with PBS by centrifugation, dehydrated through a graded ethanol series (30%–100%), and air-dried on silicon wafers (Siegert Wafer, N-doped with a

resistivity <0.005 Ω cm). SEM imaging was performed using ZEISS SUPRA 25. Image analysis was performed using ImageJ software while spectra were analyzed and normalized using Microsoft Excel.

All experiments were performed in triplicates and data are presented as mean ± standard deviation.

3. Results and Discussion

3.1 Graphene oxide promotes irreversible methylene blue aggregation and concentration-dependent quenching

GO is a water-soluble carbon-based material that can aggregate in different buffer systems as a result of ions bound to its surface (20). This inherent instability can be exploited in several physical and chemical strategies for applications such as wastewater treatment and bacteria or nucleic acid precipitation and concentration (26). Physical methods for wastewater treatment such as adsorption, and chemical processes including coagulation and flocculation, can benefit from the reactivity of GO. In addition, GO itself exhibits intrinsic catalytic properties that enable the deactivation of methylene blue and other dyes (21), mainly due to electrostatic interactions between its negatively charged surface and the positively charged dye molecules, as well as π–π interactions (40). Among graphene-based materials, GO was selected because it combines high water dispersibility with abundant oxygen-containing functional groups, including hydroxyl, epoxy, and carboxyl moieties. These surface functionalities provide a negatively charged interface that efficiently adsorbs cationic molecules such as methylene blue through electrostatic interactions and π–π stacking, while simultaneously promoting interactions with bacterial cell envelopes. In contrast, pristine graphene is highly hydrophobic and poorly dispersible in aqueous media, limiting its applicability in water treatment without additional functionalization.

Though highly water soluble, in the presence of MB, GO immediately collapses into aggregates due to electrostatic attraction between GO and the MB dye. In Figure 1, a representative picture of GO samples (100 μg/mL) soon after incubation with MB at dye concentrations ranging from 0 to 125 μg/mL.

Representative SEM images of diluted samples (Figure 1B) show a larger flake size of GO-MB (31 μg/mL), as confirmed by Dynamic Light Scattering measurements, which report an average hydrodynamic diameter of 1580 ± 113 nm for GO and 6635 ± 1210 nm for GO-MB. Zeta potential confirms that the probe is adsorbed on GO since the surface charge of GO-MB is -9.45 ± 3.66 mV compared to -25 ± 1.55 mV for pristine GO, due to the cationic nature of MB probe (41).

Representative absorption spectra characterizing MB (31 μg/mL) with or without GO in solution (25-50-100 μg/mL) are shown in Figure 1C. A comparison of probe emission immediately after mixing with GO and after 24 hours of incubation in the dark is reported. MB exists in aqueous solution as a dynamic equilibrium between monomeric and aggregated species, with the relative abundance strongly depending on dye concentration, ionic strength, and temperature. At low concentrations, the monomer predominates and exhibits a characteristic absorption maximum around 664 nm. As concentration increases, MB molecules undergo self-association through π–π stacking interactions, leading initially to the formation of dimers, which display a blue-shifted absorption band centered at approximately 610 nm (42,43). This concentration-dependent equilibrium is particularly relevant when interpreting adsorption experiments involving GO. Changes in the relative proportions of monomeric and aggregated MB species produce characteristic variations in the absorption spectrum, including the progressive increase of the dimer-associated band around 610 nm together with the decrease of the monomer peak at 664 nm. Consequently, spectral modifications should not be interpreted solely as changes in dye concentration but also as possible alterations in the aggregation state induced by adsorption onto GO surfaces.

Absorption peaks are quenched with increasing GO concentration, however, after 24 hours at 37°C, MB signal quenching in presence of GO occurs only to a limited extent, as shown by the 610 nm signal reported in Figure 1D. The persistence of the 610 and 664 nm absorption bands together with the spectral broadening below 610 nm suggests that GO does not quench MB uniformly but may also promote or stabilize higher-order aggregated species of MB on its surface, i.e. MB dimers. This behavior is consistent with the

multifunctional nature of GO, whose oxygen-containing functional groups and π-conjugated domains enable simultaneous adsorption and possible surface-mediated transformations, as reported for metal-free carbocatalytic systems (44).

To analyze the dye on GO flakes, centrifugation was performed to separate pellets and supernatants (Figure 1E) and the absorbance of supernatants (610 nm) was quantified (Figure 1F). The reduced absorbance compared to original probe signal again confirms MB binding on GO. The increase in MB retention within the pellet when increasing probe concentration can be attributed to enhanced adsorption and/or aggregation phenomena. Indeed, when MB concentration is in excess, the high local dye density might promote intermolecular interactions and increase the carbon material aggregation. This phenomenon, in turn, favors partitioning of MB into GO-associated sedimented phase. On the whole, these data indicate a measurable degree of surface adsorption and limited quenching of GO proportionally to available GO surface, i.e. to GO concentration.

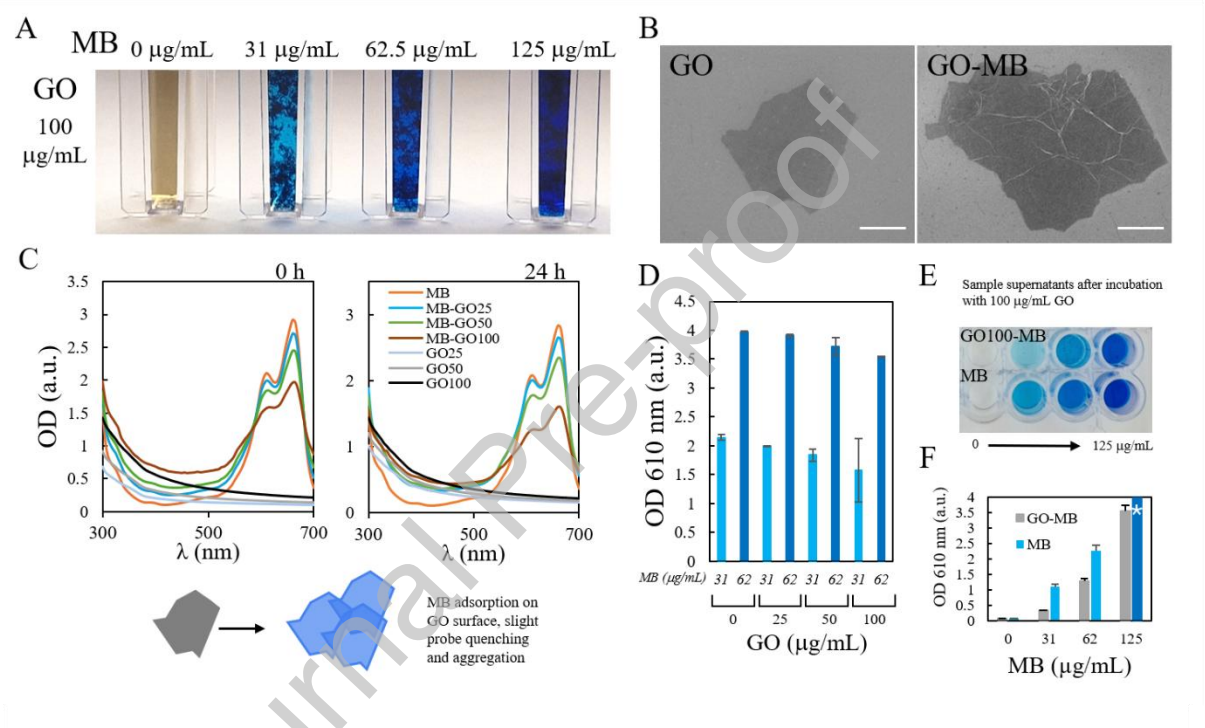

Figure 1. Characterization of GO–MB samples and adsorption of MB. (A) Photographs of MB solutions at increasing concentrations (0–125 µg/mL) in the presence of graphene oxide (GO, 100 µg/mL), showing the GO aggregation. (B) Representative SEM micrographs of GO sheets and GO–MB complexes, scale bar is 1 µm (C) Optical Density (OD) recorded at 0 h and 24 h for MB solutions incubated with different concentrations of GO (25, 50, and 100 µg/mL). The characteristic MB absorption peaks at 610 nm and 664 nm are visible. (D) Quantification of the absorbance at 610 nm for MB solutions incubated with different GO concentrations (0-25-50-100 µg/mL). (E) Representative images and (F) quantitative analysis of the supernatants after incubation with 100 µg/mL GO, showing reduced MB concentration in solution as measured by the absorbance at 610 nm.

3.2 *E. coli* can precipitate MB in dark, but is sensitive to MB toxicity

E. coli is not known as an efficient microorganism for dye degradation, being neither exoelectrogenic nor a typical decolorizing bacterium. When *E.coli* is incubated with MB, a significant fraction of dye was found to be associated with the bacterial pellet after 24 hours, leading to a reduced signal in the corresponding supernatants (Figure 2A, third row). Spectroscopic analysis of the supernatants (Figure 2B) revealed a parallel decrease in absorbance at both 610 nm and 664 nm, without significant variation in their intensity ratio, suggesting that free dye is not modified by bacteria.

On the contrary, spectra acquired from whole samples (Figure 2C) show a marked redistribution of spectral features. In particular, after 24 hours, a depletion of the 664 nm band, associated with monomeric MB, is observed together with a slight blue shift and a pronounced increase and broadening of the band centered

around 610 nm. This behavior suggests a time-dependent stabilization of dimeric and possibly higher-order aggregated MB species, promoted by interactions with *E. coli* cell surfaces. The phenomenon is visible only at 31 µg/mL. At a concentration of 62 µg/mL, a global decrease in peak height occurs, with no modification of monomeric/dimeric proportion. This is probably due to toxicity effects on *E.coli*. Indeed, CFU assay confirms that at high MB concentrations (>62 µg/mL), *E. coli* is not viable after 24 hours of incubation (Figure 2D), in agreement with literature values (45). On the whole these data demonstrate that MB is associated with bacterial cells due to precipitation in the sample pellet and that when MB concentration is low and toxicity is not complete, the active metabolism of *E. coli* changes probe state.

Due to spectra saturation and high toxicity towards bacteria, the 125 µg/mL concentration has been excluded from subsequent experiments.

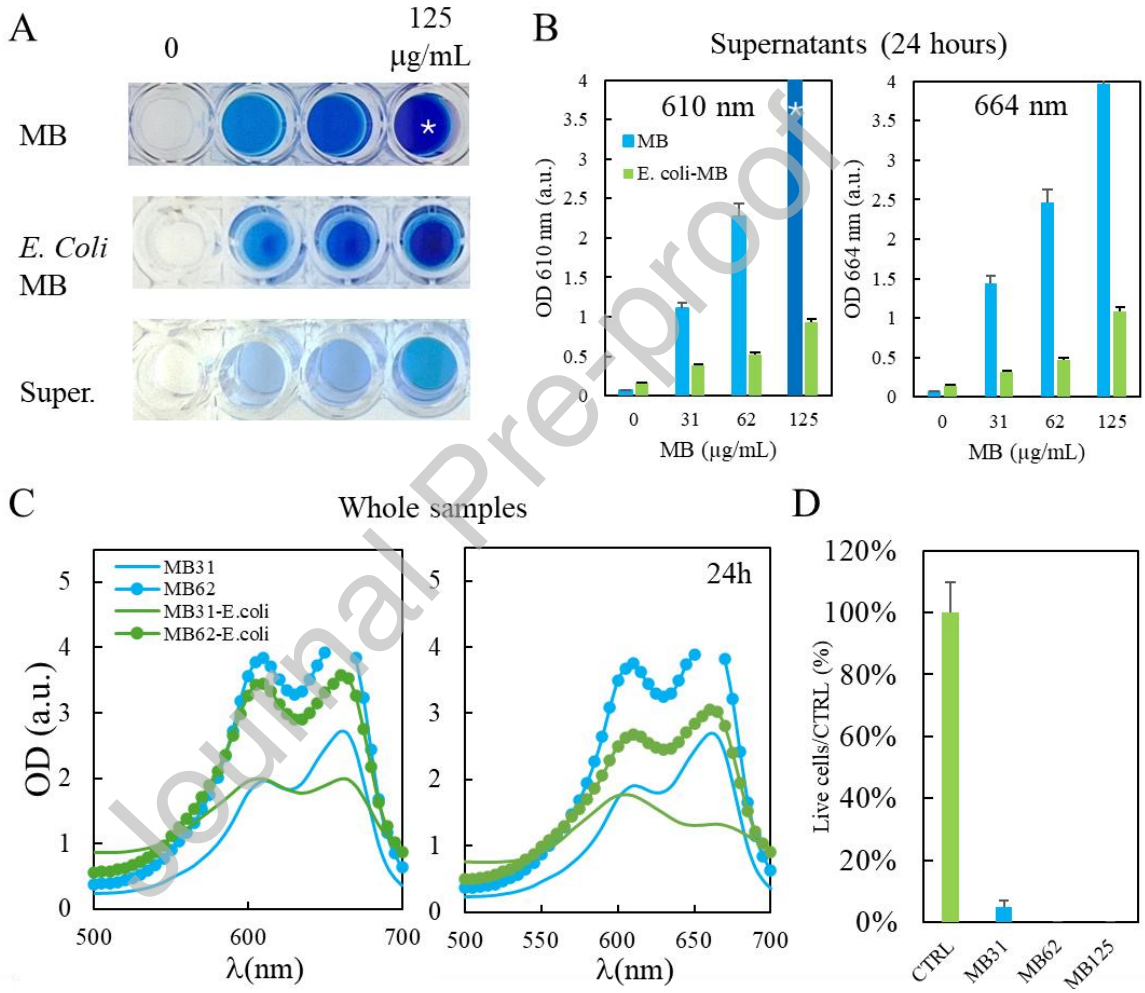

Figure 2 Interaction of MB with *E. coli* after 24 h incubation. (A) Representative images of MB solutions at increasing concentrations (0–125 µg/mL) in the absence and presence of *E. coli*, before and after centrifugation. The formation of a blue pellet indicates MB association with bacterial cells. (B) Quantification of MB in supernatants after centrifugation, showing a concentration-dependent decrease in absorbance at 610 nm and 664 nm in the presence of *E. coli*, without significant changes in their ratio. (C) UV–Vis absorption spectra of whole samples at 0 h and after 24 h incubation. In the presence of *E. coli*, a decrease of the 664 nm band and a blue shift with increased intensity and broadening of the ~610 nm band are observed, consistent with the formation and stabilization of aggregated MB species. (D) CFU results obtained treating cells with increasing MB concentration.

3.3 The synergistic effect between *E. coli* and GO causes a higher MB removal due to confinement and surface contact

The combined effect of GO and *E. coli* on MB was investigated by incubating samples at 37 °C in the dark using a fixed GO concentration of 100 µg/mL in water without nutrients. The formation of GO–bacteria

aggregates is clearly visible in the sample photographs (Figure 3A) and confirmed by SEM imaging (Figure 3B), showing close physical association between GO sheets and bacterial cells in both undiluted and diluted samples (left and right images in Figure 3B, respectively). At this concentration a repulsive interaction between GO flakes is expected in water. UV–Vis absorption spectra recorded immediately after mixing or after 24 h of incubation are reported in Figure 3C for MB concentrations of 31 and 62 µg/mL, in the presence of GO and/or *E. coli*. The absorbance profiles are significantly affected when both GO and bacterial cells are present. In the presence of GO alone, a general decrease in absorbance intensity is observed over the whole spectral range, consistent with MB adsorption onto GO surface and associated quenching effects reported in Figure 1. The presence of *E. coli* leads to a pronounced redistribution of spectral features at 31 µg/mL, as discussed above. When GO and *E. coli* are combined, the spectral response reflects a synergistic effect. A strong overall decrease in absorbance is observed, due to enhanced MB removal from solution, together with a clear broadening and relative enhancement of the band below ~610 nm. This behaviour suggests that GO–bacteria aggregates provide a heterogeneous interface that promotes MB accumulation and stabilizes dimeric and higher-order aggregated species associated to bacteria membrane. Notably, after 24 h, all systems containing *E. coli* and GO show decreased spectra intensity, with the effect more pronounced at higher MB concentration (62 µg/mL) (Figure 3C).

Since visible precipitation was observed, the distribution of MB between pellet and supernatant was quantified after centrifugation, and the possibility of probe release upon washing was evaluated. As shown in Figure 3D, *E. coli* adsorbs most of the probe at 31 µg/mL, while its efficiency decreases at 62 µg/mL, likely due to increased toxicity at higher dye concentration. GO alone shows relatively low adsorption overall, consistent with previous observations, and its uptake scales with MB concentration, reflecting the availability of adsorption sites. In the presence of the nanomaterial and bacteria, MB undergoes adsorption together with a reduction of its detectable absorbance, as suggested by the disappearance of the signal from both pellet and supernatant in the GO100–*E. coli*–MB31 condition (Figure 3D). At 62 µg/mL, although a larger fraction of MB is associated with the pellet, the removal appears less efficient, indicating that higher MB concentrations may inhibit bacterial activity also in presence of GO. To demonstrate this hypothesis, the addition of Ca^{2+} was used to promote the separation between GO, bacterial cells, and free MB. Calcium ions are indeed known to screen electrostatic interactions and induce tight aggregation of GO sheets and bacterial membranes, i.e. competing with MB for surface binding (38). Under these experimental conditions, it was observed that Ca^{2+} promotes aggregation of GO flakes and enhances the precipitation of GO–MB complexes at both 31 and 62 µg/mL. When *E. coli* is present, the bacterial surface appears to be partially screened by Ca^{2+} ions and GO aggregates, leading to (i) a higher fraction of MB in the supernatant and (ii) an increased signal of MB that precipitates in the pellet. Indeed, the pellet signal becomes comparable to that observed for *E. coli* with MB (Figure 3D). A plausible explanation is that Ca^{2+} reduces electrostatic interactions between MB and negatively charged bacterial membranes, while simultaneously favours GO-driven aggregation. As a result, MB partitioning becomes dominated by physical entrapment rather than active bacterial surface transformation, explaining the loss of synergistic effects in these conditions.

To provide a quantitative estimate of dye removal under the tested conditions, the removal efficiency was calculated from the absorbance of the supernatants at 610 nm. The calculated values confirmed that the combined GO–*E. coli* system achieved the highest MB removal efficiency under nutrient-free conditions (Figure 3E). An apparent adsorption capacity $q_e$was calculated by normalizing the amount of removed MB to the GO mass. The apparent MB removal capacity increased with the initial dye concentration in both GO-containing systems. For GO alone, the calculated capacity increased from 199.9 to 264.6 mg g^{-1} when the initial MB amount was increased from 31 to 62 µg. In the presence of E. coli, the corresponding values increased from 268.0 to 592.0 mg g^{-1}. Thus, bacterial addition enhanced the apparent removal capacity by approximately 34% at the lower MB concentration and by 124% at the higher concentration. The markedly stronger enhancement observed at 62 µg MB suggests that the contribution of the bacterial component becomes increasingly relevant under conditions in which the adsorption capacity of GO alone begins to be limiting. Since these values were normalized to the GO mass, they should be interpreted as apparent removal capacities of the hybrid system rather than as intrinsic equilibrium adsorption capacities of GO. The enhanced performance of the GO–*E. coli* system is consistent with the formation of a confined bio–nano interface. We hypothesize that this localized microenvironment may increase the local concentration of MB at the bacterial surface and thereby facilitate adsorption and/or membrane-associated transformation processes that might be elucidated in proteomic or genomic studies in the future.

To verify the strength of bonding the pellets were washed in fresh ultrapure water and the released MB was quantified (Figure 3F). Washing experiments indicate that only a limited fraction of MB is released back into the supernatant, suggesting that interactions between MB and pellet components are relatively strong and only partially reversible. Notably, the lowest release values are observed for the combined *E. coli*–GO system, whereas the highest release occurs in the presence of Ca^{2+}. As expected, the amount of released MB is higher at 62 µg/mL, where the binding efficiency is reduced across all conditions. Nevertheless, the *E. coli*–GO combination consistently shows superior retention, confirming a cooperative effect on MB decolorization which is impeded in presence of divalent ions.

To investigate the fate of MB associated with GO, the pellets were treated with a desorption solution containing 50% ethanol and 0.1 M HCl. Although the treatment detached MB from the GO surface, the recovered absorbance remained markedly lower than that of free MB or the *E. coli*-only control (Figure 3G). This finding suggests that a fraction of the dye lost its original spectroscopic properties while associated with the GO-containing aggregates. Therefore, the reduced signal after desorption cannot be explained solely by incomplete dye recovery but is also consistent with a partial loss of the spectroscopic properties of methylene blue during the interaction with the GO–*E. coli* system.

GO-MB aggregation appears to improve bacterial viability, likely by reducing direct membrane damage caused by MB dye. It can be hypothesized that by increasing GO concentration a further improvement of detoxification occurs. However, GO is toxic at high concentration, and the limitation of bacterial viability induces a loss of enzymatic activity. To verify toxicity, bacterial viability was evaluated in the presence of GO at higher concentration (200 µg/mL). Indeed, the toxicity of GO itself reaches ~84% and the improvement of MB effect remains limited (Figure 3H). A concentration of 100 µg/mL represents therefore an optimal compromise, providing a large available surface area for MB adsorption while maintaining sufficient bacterial viability, an important aspect for scalability in batch processes.

Overall, these data support a model in which MB is removed from solution through combined adsorption onto GO, bacterial cells, and GO–bacteria aggregates, with limited release upon washing and minimal contribution from irreversible chemical sequestration (Scheme in Figure 3I). A possible contribution of membrane-associated enzymes can be hypothesized, potentially facilitated by the close proximity between GO sheets and bacterial cells, which may enhance local MB concentration at the cell surface and promote enzymatic transformation. However, this mechanism requires further genetic investigation.

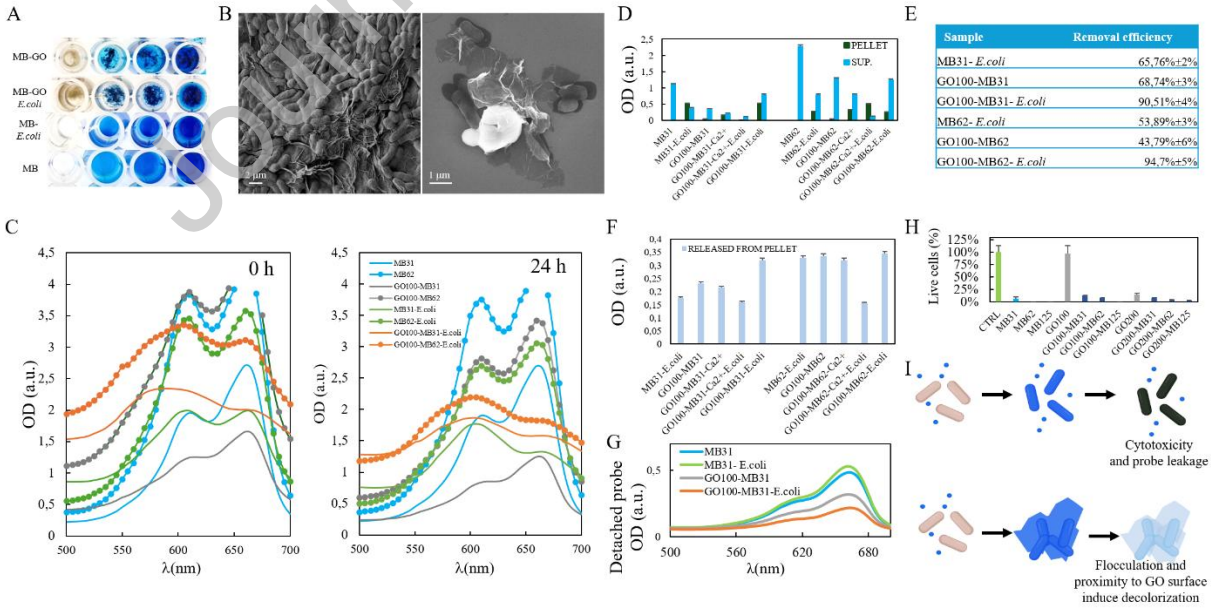

Figure 3. Combined effect of GO and *E. coli* on MB adsorption and spectral behaviour. (A) Representative images of MB solutions (31, 62, 125 µg/mL) in the presence of GO (100 µg/mL) and/or *E. coli*, showing the formation of visible GO–bacteria aggregates. (B) SEM images of GO–bacteria assemblies, highlighting the close interaction between GO sheets and *E. coli* cells. V(C) UV–Vis absorption spectra of MB solutions immediately after mixing (left) and after 24 h incubation at 37 °C in the dark (right). GO

induces a general decrease in absorbance due to MB adsorption, while *E. coli* promotes a redistribution of spectral features with a decrease of the 664 nm band and an increase and broadening of the ~610 nm band. The combined GO–*E. coli* system exhibits enhanced MB removal and stabilization of aggregated species, particularly after 24 h. (D) Distribution of MB between pellet and supernatant after centrifugation, highlighting the contribution of GO, *E. coli*, and their combination to probe sequestration. *E. coli* shows higher adsorption efficiency at 31 µg/mL, which decreases at 62 µg/mL, while GO alone exhibits limited uptake proportional to dye concentration. The combined system results in enhanced MB retention in the pellet, suggesting a synergistic effect. The addition of Ca^{2+} promotes aggregation and phase separation, leading to increased pellet-associated signal and altered partitioning of MB between pellet and supernatant. (E)Removal efficiency of GO calculated from supernatants (F) Fraction of MB released from the pellet after washing, indicating that only a limited amount of dye is recovered in the supernatant. The lowest release is observed for the GO–E. coli system, whereas higher release occurs in the presence of Ca^{2+} and at higher MB concentration, consistent with weaker binding interactions. (G) UV–Vis absorption spectra of methylene blue (MB) recovered from GO-containing pellets after desorption with 50% ethanol and 0.1 M HCl. (H) Bacterial viability expressed as percentage of live cells relative to control (CTRL) under the different experimental conditions, showing that GO concentration and aggregation state influence E. coli survival. GO at 100 µg/mL allows partial preservation of viability while maintaining adsorption performance, whereas higher concentrations lead to increased cytotoxicity. (I) The formation of GO–bacteria aggregates enables efficient MB sequestration.

3.4 NIR light can be used to stop bacteria growth after MB-GO precipitation

Bacterial uncontrolled growth should be avoided during microorganisms-based environmental application. To ensure biocontainment after detoxification, we designed a strategy based on NIR adsorption properties of GO. Indeed, when a NIR laser is focused on GO, the absorbed photons are converted into thermal energy, leading to a localized temperature increase. This photothermal effect can disrupt bacterial cell membranes and denature vital biomolecules, thereby enhancing the antibacterial activity of GO (46). We investigated whether NIR treatment could inhibit bacterial growth after long term GO and MB (31 µg/mL) bacterial confinement. To do so, we exposed GO–*E. coli* or GO-MB–*E.coli* aggregates at to two different NIR laser powers and evaluated bacterial survival. For comparison also MB- *E.coli* or untreated *E.coli* were irradiated. The average maximum temperature of GO samples at the highest power was 49 °C, while GO-MB reached a maximum of 53.5 °C in 240 seconds, due to the ability of MB to act as photothermal absorber itself (Figure 4A). CFU analysis shows that, as expected, GO-MB can improve viability of *E.coli* thanks to MB detoxification. In particular, after 72 hours, 40% living cells have been recovered in the sample. When irradiated with NIR at low laser power GO-MB adsorption of light induces increase of temperature and cell death, at higher laser power also GO alone is effective in cell killing, demonstrating the ability to control long term bacteria growth (Figure 4B). Representative CFU plates of different treatments and NIR high power effects are reported in Figure 4C.

A possible contribution of membrane-associated enzymes can be hypothesized, but no direct evidence is provided in the present study. The contribution of bacterial metabolism, specific enzymatic pathways, oxidative species generation, or transcriptional responses cannot be established from the current dataset and will require dedicated studies.

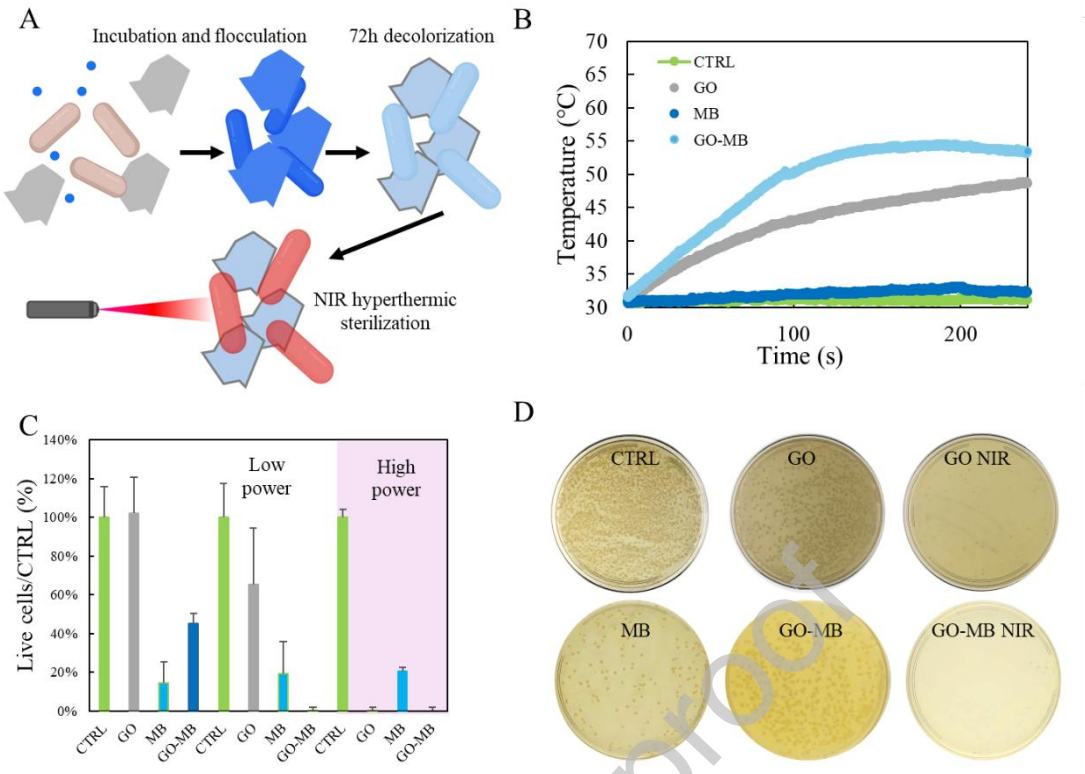

Figure 4 Viability of *E. coli* after treatment with MB or GO–MB and effects of NIR irradiation as illustrated in scheme in (A). (B) Temperature profiles recorded during near-infrared (NIR) irradiation for CTRL, GO, MB, and GO–MB samples, showing the photothermal effect of GO-based materials. (C) Normalized colony-forming units (CFU) after NIR irradiation at low and high-power conditions, indicating enhanced antibacterial activity under higher irradiation power. (D) Representative pictures of *E. coli* colonies grown on agar plates after the different treatments (CTRL, GO, GO + NIR, MB, GO–MB, and GO–MB + NIR), illustrating the reduction in bacterial growth following GO–MB treatment combined with NIR high power exposure.

Table 1 Comparison of representative graphene-based and biological strategies for methylene blue removal from aqueous solutions

Study	Material	Microorganism	Metal catalyst	Light required	Main removal mechanism	MB adsorption/removal performance
Yan et al. (31)	GO	No	No	No	Adsorption	GO adsorption strongly depends on oxidation degree
Jahan et al. (29)	GO/rGO	No	No	No	Adsorption	GO exhibited higher adsorption capacity
Arias et al.(32)	Green rGO	No	No	No	Adsorption	High MB adsorption capacity
Mahich et al.(30)	GO/rGO	No	No	No	Adsorption + photocatalysis	Enhanced removal under light irradiation
Moradi et al. (25)	GO/CuO composite	No	Yes	Yes	Adsorption + catalysis	Efficient dye removal but requires metal catalyst

Unlike previous graphene-based systems that mainly rely on adsorption or photocatalysis, the present work demonstrates that commercially available pristine graphene oxide and wild-type E. coli spontaneously cooperate under nutrient-free and light-independent conditions, providing enhanced MB removal through bio–nano flocculation.

4. Conclusions

Conventional metal-based photocatalysts, although effective, may suffer from high costs and the risk of secondary metal contamination, highlighting the need for metal-free alternatives such as graphene oxide-based systems (20). This study demonstrates that the combination of GO and *E. coli* enables an efficient light-independent removal of MB from water through a cooperative mechanism involving adsorption, aggregation, and confinement of the dye within GO–bacteria flocs. While GO-induced flocculation of dyes has been previously reported (41), here we demonstrate that the presence of bacterial cells promotes the formation of hybrid bio–nano aggregates that enhance dye retention and transformation. Compared to GO or bacterial cells alone, the hybrid system provides enhanced MB sequestration, reduced release after washing, and improved retention of the dye in the pellet phase, indicating the establishment of relatively strong and only partially reversible interactions. A key outcome of this work is that GO at 100 µg/mL provides a favourable compromise between adsorption capacity and bacterial viability. Under these conditions, GO-mediated confinement appears to mitigate part of the toxic effects of MB on *E. coli*, while still enabling bacteriostatic control of the final GO–MB–bacteria assembly. This is particularly relevant for scalable batch-based water treatment processes, where maintaining a sufficient degree of microbial activity without uncontrolled proliferation is essential. In this respect, the possibility of terminating the process by near-infrared irradiation adds an important level of operational control and biocontainment.

From an environmental standpoint, the proposed GO–*E. coli* platform offers relevant advantages, including operation in water and in the dark, the absence of added metal catalysts or oxidants, a reduced need for auxiliary reagents, and the possibility of limiting secondary inorganic contamination. Compared with conventional dye-removal routes, which often involve high chemical demand, sludge generation, and additional post-treatment requirements based on photocatalysis, this hybrid approach relies on spontaneous bioflocculation and adsorption-driven confinement of the pollutant, in line with the need for more sustainable wastewater treatment technologies (2,36,37). In addition, the use of a carbon-based adsorbent such as GO is consistent with the growing interest in nanomaterial-enabled platforms for wastewater remediation, valued for their high surface area and tunable interfacial properties (36,47), while the incorporation of a microbial component further supports process sustainability by enabling operation under mild conditions without external energy input or nutrient supplementation.

Importantly, while the present data support the existence of a synergistic interaction between GO and living E. coli cells, the molecular basis of this effect remains unresolved. The possible involvement of membrane-associated enzymes, bacterial metabolism, or ROS-mediated reactions remains speculative and was not directly investigated in this proof-of-concept study. Future work including metabolic inhibition assays, heat-killed controls, enzyme inhibition, ROS measurements, and transcriptomic/proteomic analyses will be required to elucidate the underlying mechanism.

By combining the adsorption capacity of graphene oxide with the adaptive properties of bacterial cells, while maintaining the possibility of post-treatment bacterial inactivation by NIR irradiation, this hybrid strategy represents a promising step toward more sustainable and controllable carbon-based bioremediation systems for dye-polluted waters. From an application perspective, the spontaneous formation of visible GO–E. coli flocs may facilitate their recovery from treated water by conventional sedimentation or low-speed centrifugation, simplifying post-treatment separation(22). However, the stability and recovery of these aggregates in complex environmental waters containing competing ions and natural organic matter remain to be investigated before practical implementation. Future work will be directed toward optimizing the surface chemistry of graphene oxide to modulate its interaction with dyes and bacterial cells, and toward engineering

E. coli strains with improved metabolic capabilities, in order to further enhance the performance and applicability of this hybrid bio–nano remediation strategy.

Acknowledgements

This work received funding from the Italian Ministry of University and Research (MIUR), "One Health Basic and Translational Research Actions addressing Unmet Needs on Emerging Infectious Diseases—INFACT"—PNRR NextGenerationEU (project code: PE00000007, CUP B53C20040570005) - Missione 4 "Istruzione e Ricerca" - Componente C2; Investimento 1.3 funded by the Italian Ministry of University and Research.

References

1. Sarwar T, Khan S. Textile industry: pollution health risks and toxicity. Text Wastewater Treat Sustain Bio-nano Mater Macromol Vol 1. Springer; 2022. page 1–28.
2. Mazotto AM, de Ramos Silva J, de Brito LAA, Rocha NU, de Souza Soares A. How can microbiology help to improve sustainability in the fashion industry? Environ Technol Innov. Elsevier; 2021;23:101760.
3. Lellis B, Fávaro-Polonio CZ, Pamphile JA, Polonio JC. Effects of textile dyes on health and the environment and bioremediation potential of living organisms. Biotechnol Res Innov. Elsevier; 2019;3:275–90.
4. Przystaś W, Zabłocka-Godlewska E, Grabińska-Sota E. Biological removal of azo and triphenylmethane dyes and toxicity of process by-products. Water, Air, Soil Pollut. Springer; 2012;223:1581–92.
5. Chakraborty B, Ray L, Basu S. Biochemical degradation of Methylene Blue using a continuous reactor packed with solid waste by E. coli and Bacillus subtilis isolated from wetland soil. Desalin Water Treat. Taylor & Francis; 2016;57:14077–82.
6. Sarkar S, Banerjee A, Halder U, Biswas R, Bandopadhyay R. Degradation of synthetic azo dyes of textile industry: a sustainable approach using microbial enzymes. Water Conserv Sci Eng. Springer; 2017;2:121–31.
7. Romero S, Blánquez P, Caminal G, Font X, Sarrà M, Gabarrell X, et al. Different approaches to improving the textile dye degradation capacity of Trametes versicolor. Biochem Eng J. Elsevier; 2006;31:42–7.
8. Singh RL, Singh PK, Singh RP. Enzymatic decolorization and degradation of azo dyes–A review. Int Biodeterior Biodegradation. Elsevier; 2015;104:21–31.
9. Pinheiro LRS, Gradíssimo DG, Xavier LP, Santos AV. Degradation of azo dyes: bacterial potential for bioremediation. Sustainability. MDPI; 2022;14:1510.
10. Kapoor RT, Danish M, Singh RS, Rafatullah M, HPS AK. Exploiting microbial biomass in treating azo dyes contaminated wastewater: Mechanism of degradation and factors affecting microbial efficiency. J Water Process Eng. Elsevier; 2021;43:102255.
11. Aragaw TA. A review of dye biodegradation in textile wastewater, challenges due to wastewater characteristics, and the potential of alkaliphiles. J Hazard Mater Adv. Elsevier; 2024;16:100493.
12. Kuc ME, Azerrad S, Menashe O, Kurzbaum E. Efficient biodegradation of phenol at high concentrations by Acinetobacter biofilm at extremely short hydraulic retention times. J Water Process Eng. Elsevier; 2022;47:102781.
13. Gu Q, Wu Q, Zhang J, Guo W, Wu H, Sun M. Community analysis and recovery of phenol-degrading bacteria from drinking water biofilters. Front Microbiol. Frontiers Media SA; 2016;7:495.
14. Maurya VK, Kumar S, Prasad AK, Bhatt MLB, Saxena SK. Structure-based drug designing for

potential antiviral activity of selected natural products from Ayurveda against SARS-CoV-2 spike glycoprotein and its cellular receptor. Virusdisease. Springer; 2020;31:179–93.

15. Zhuang M, Sanganyado E, Zhang X, Xu L, Zhu J, Liu W, et al. Azo dye degrading bacteria tolerant to extreme conditions inhabit nearshore ecosystems: optimization and degradation pathways. J Environ Manage. Elsevier; 2020;261:110222.

16. Chen B-Y, Chen S-Y, Lin M-Y, Chang J-S. Exploring bioaugmentation strategies for azo-dye decolorization using a mixed consortium of Pseudomonas luteola and Escherichia coli. Process Biochem. Elsevier; 2006;41:1574–81.

17. Dixit S, Garg S. Development of an efficient recombinant bacterium and its application in the degradation of environmentally hazardous azo dyes. Int J Environ Sci Technol. Springer; 2019;16:7137–46.

18. Jin R, Yang H, Zhang A, Wang J, Liu G. Bioaugmentation on decolorization of CI Direct Blue 71 by using genetically engineered strain Escherichia coli JM109 (pGEX-AZR). J Hazard Mater. Elsevier; 2009;163:1123–8.

19. Ruan W, Hu J, Qi J, Hou Y, Zhou C, Wei X. Removal of dyes from wastewater by nanomaterials: a review. Adv Mater Lett. 2019;10:9–20.

20. Thakur S, Bi A, Mahmood S, Ruzimuradov O, Gupta R, Cho J, et al. Graphene oxide as an emerging sole adsorbent and photocatalyst: Chemistry of synthesis and tailoring properties for removal of emerging contaminants. Chemosphere. Elsevier; 2024;352:141483.

21. Palmieri V, de Spirito M, Papi M. Enhanced Microbial Sensing via Resazurin Reduction Catalyzed by Graphene Oxide, A Versatile Approach for Diagnostics and Electrochemical Applications. Environ Toxicol. Wiley Online Library; 2025;

22. Yang J, Yan X, Qin Y, Zhang D, Zhao J, Yu Y, et al. Magnetic-field-free separation and recovery of MXene-doped GO composites via dye-bridged reassembly in dye adsorption. RSC Adv. 2026;16:29576.

23. Moradi A, Kalaee MR, Moradi O, Mohammad Mahmoodi N, Zaarei D. Novel Binary and Ternary Biocomposites (Zeolitic Imidazolate Framework (ZIF-67), Graphene Oxide (GO) Nanosheet, and Guar Gum (GG) Biopolymer): Synthesis and Adsorption of Malachite Green Cationic Dye. ChemistrySelect. Wiley Online Library; 2025;10:e202404673.

24. Naeini AH, Kalaee MR, Moradi O, Khajavi R, Abdouss M. Synthesis, characterization and application of carboxylmethyl cellulose, guar gam, and graphene oxide as novel composite adsorbents for removal of malachite green from aqueous solution. Adv Compos Hybrid Mater. Springer; 2022;5:335–49.

25. Moradi O, Mirzaian M, Sedaghat S. Poly (methyl methacrylate) functionalized graphene oxide/CuO as nanocomposite for efficient removal of dye pollutants. Sci Rep. Nature Publishing Group UK London; 2024;14:22318.

26. Moradi O, Madanpisheh MA, Moghaddas M. Synthesis of GO/HEMA, GO/HEMA/TiO2, and GO/Fe3O4/HEMA as novel nanocomposites and their dye removal ability. Adv Compos Hybrid Mater. Springer; 2021;4:1185–204.

27. Behzad N, Moradi O, Raissi H, Hakimi M, Mozaffari S. Synthesis of graphene oxide–magnesium oxide composites and cationic dyes removal from water. Desalin Water Treat. Elsevier; 2023;300:213–29.

28. Moradi O, Pudineh A, Sedaghat S. Synthesis and characterization Agar/GO/ZnO NPs nanocomposite for removal of methylene blue and methyl orange as azo dyes from food industrial effluents. Food Chem Toxicol. Elsevier; 2022;169:113412.

29. Jahan N, Roy H, Reaz AH, Arshi S, Rahman E, Firoz SH, et al. A comparative study on sorption

behavior of graphene oxide and reduced graphene oxide towards methylene blue. Case Stud Chem Environ Eng. Elsevier; 2022;6:100239.

30. Mahich S, Saini YK, Devra V, Aggarwal K, Kumar A, Kumar D, et al. Metal-free adsorption and photodegradation methods for methylene blue dye removal using different reduction grades of graphene oxide. Heliyon. Elsevier; 2024;10.

31. Yan H, Tao X, Yang Z, Li K, Yang H, Li A, et al. Effects of the oxidation degree of graphene oxide on the adsorption of methylene blue. J Hazard Mater. Elsevier; 2014;268:191–8.

32. Arias Arias F, Guevara M, Tene T, Angamarca P, Molina R, Valarezo A, et al. The adsorption of methylene blue on eco-friendly reduced graphene oxide. Nanomaterials. MDPI; 2020;10:681.

33. Palmieri V, Bugli F, Lauriola MC, Cacaci M, Torelli R, Ciasca G, et al. Bacteria Meet Graphene: Modulation of Graphene Oxide Nanosheet Interaction with Human Pathogens for Effective Antimicrobial Therapy. ACS Biomater Sci Eng. 2017;3:619–27.

34. De Maio F, Palmieri V, Salustri A, Perini G, Sanguinetti M, De Spirito M, et al. Graphene Oxide Prevents Mycobacteria Entry in Macrophages Through Extracellular Entrapment. Nanoscale Adv. Royal Society of Chemistry; 2019;

35. De Maio F, Palmieri V, Babini G, Augello A, Palucci I, Perini G, et al. Graphene nanoplatelet and Graphene oxide functionalization of face mask materials inhibits infectivity of trapped SARS-CoV-2. Iscience. Elsevier; 2021;24:102788.

36. Anegbe B, Ifijen IH, Maliki M, Uwidia IE, Aigbodion AI. Graphene oxide synthesis and applications in emerging contaminant removal: a comprehensive review. Environ Sci Eur. Springer; 2024;36:15.

37. Al-Tohamy R, Ali SS, Li F, Okasha KM, Mahmoud YA-G, Elsamahy T, et al. A critical review on the treatment of dye-containing wastewater: Ecotoxicological and health concerns of textile dyes and possible remediation approaches for environmental safety. Ecotoxicol Environ Saf. Elsevier; 2022;231:113160.

38. Palmieri V, Bugli F, Lauriola MC, Cacaci M, Torelli R, Ciasca G, et al. Bacteria meet graphene: modulation of graphene oxide nanosheet interaction with human pathogens for effective antimicrobial therapy. ACS Biomater Sci Eng. ACS Publications; 2017;3:619–27.

39. Palmieri V, Amato F, Marrani AG, Friggeri G, Perini G, Augello A, et al. Graphene oxide-mediated copper reduction allows comparative evaluation of oxygenated reactive residues exposure on the materials surface in a simple one-step method. Appl Surf Sci. Elsevier; 2023;156315.

40. Soudagar S, Akash S, Venkat MS, Poiba VR, Vangalapati M. Adsorption of methylene blue dye on nano graphene oxide-thermodynamics and kinetic studies. Mater Today Proc. Elsevier; 2022;59:667–72.

41. Liu J, Li P, Xiao H, Zhang Y, Shi X, Lü X, et al. Understanding flocculation mechanism of graphene oxide for organic dyes from water: Experimental and molecular dynamics simulation. AIP Adv. AIP Publishing; 2015;5.

42. Fernández-Pérez A, Valdés-Solís T, Marbán G. Visible light spectroscopic analysis of Methylene Blue in water; the resonance virtual equilibrium hypothesis. Dye Pigment. Elsevier; 2019;161:448–56.

43. Fernández Pérez A, Marbán Calzón G. Visible light spectroscopic analysis of methylene blue in water; what comes after dimer? American Chemical Society; 2020;

44. Gao F, Zhang S, Lv Q, Yu B. Recent advances in graphene oxide catalyzed organic transformations. Chinese Chem Lett. Elsevier; 2022;33:2354–62.

45. Sabbahi S, Alouini Z, Ayed L Ben, Jemli M. Inactivation of faecal bacteria in wastewater by methylene blue and visible light. Desalin Water Treat. Elsevier; 2010;20:209–19.

46. Friggeri G, Moretti I, Amato F, Marrani AG, Sciandra F, Colombarolli SG, et al. Multifunctional scaffolds for biomedical applications: Crafting versatile solutions with polycaprolactone enriched by graphene oxide. APL Bioeng. AIP Publishing; 2024;8.

47. Liu H, Wang B, Liu H, Zheng Y, Li M, Tang K, et al. Multi-crosslinked robust alginate/polyethyleneimine modified graphene aerogel for efficient organic dye removal. Colloids Surfaces A Physicochem Eng Asp. Elsevier; 2024;683:133034.

Author statement

Valentina Palmieri: Conceptualization, Methodology, Investigation, Formal analysis, Data curation, Writing – original draft, Supervision.

Valeria Ferrara: Investigation, Methodology, Data curation.

Caterina Perfili: Investigation.

Ginevra Friggeri: Investigation.

Giulia Artemi: Investigation.

Giordano Perini: Investigation, Formal analysis.

Alberto Augello: Investigation.

Francesca Sciandra: Materials characterization, Investigation.

Francesco Amato: Investigation, Methodology, Data curation.

Andrea Giacomo Marrani: Materials characterization, Investigation, Resources

Claudio Catalano: Investigation.

Umberto Romeo: Resources, Supervision.

Guido Caldarelli: Supervision, Funding acquisition.

Marco De Spirito: Conceptualization, Supervision, Writing – review & editing.

Massimiliano Papi: Conceptualization, Supervision, Writing – review & editing.

Graphical abstract

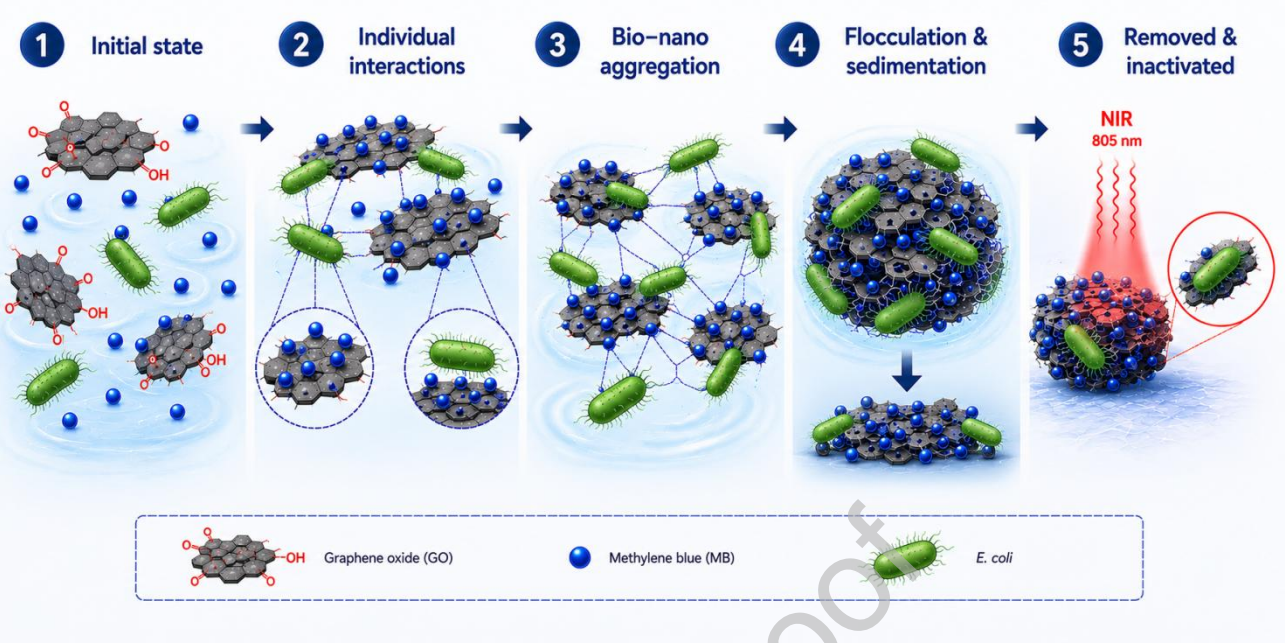

Declaration of interests

☒The authors declare that they have no known competing financial interests or personal relationships that could have appeared to influence the work reported in this paper.